Efficient Mapping and Cloning of Mutations in Zebrafish by Low-Coverage Whole-Genome Sequencing

Margot E. Bowen,*,†,1 Katrin Henke,*,†,1 Kellee R. Siegfried,* Matthew L. Warman,*,† and Matthew P. Harris*,†,2
*Orthopedic Research Laboratories, Children's Hospital, Boston, Massachusetts 02115, and †Department of Genetics, Harvard Medical School, Boston, Massachusetts 02115

ABSTRACT The generation and analysis of mutants in zebrafish has been instrumental in defining the genetic regulation of vertebrate development, physiology, and disease. However, identifying the genetic changes that underlie mutant phenotypes remains a significant bottleneck in the analysis of mutants. Whole-genome sequencing has recently emerged as a fast and efficient approach for identifying mutations in nonvertebrate model organisms. However, this approach has not been applied to zebrafish due to the complicating factors of having a large genome and lack of fully inbred lines. Here we provide a method for efficiently mapping and detecting mutations in zebrafish using these new parallel sequencing technologies. This method utilizes an extensive reference SNP database to define regions of homozygosity-by-descent by low coverage, whole-genome sequencing of pooled DNA from only a limited number of mutant F_2 fish. With this approach we mapped each of the five different zebrafish mutants we sequenced and identified likely causative nonsense mutations in two and candidate mutations in the remainder. Furthermore, we provide evidence that one of the identified mutations, a nonsense mutation in *bmp1a*, underlies the *welded* mutant phenotype.

A major strength of the zebrafish (*Danio rerio*) model is the feasibility of performing large-scale genetic screens as a means to isolate mutants to study gene function. Such forward genetic screens have led to the identification of a large collection of mutants defective in a variety of biological processes. The standard approach for identifying the responsible mutation underlying a mutant phenotype is to perform bulked segregant analysis with simple sequence length polymorphisms (SSLPs) (Geisler *et al.* 2007), followed by fine mapping using individual fish to define the region in which the mutation lies. Candidate genes within the mapped interval are then screened for the presence of mutations, typically by sequencing cDNA or genomic DNA. This approach is time and labor intensive, requiring large numbers of mutant fish and often years to successfully clone a mutant. To date this is a major limitation in zebrafish research, and large numbers of mutants have not yet been mapped or cloned.

Whole-genome sequencing (WGS) has the potential to expedite the process of mutation detection in zebrafish. In *Caenorhabditis elegans* and *Arabidopsis thaliana*, multiple studies have shown that, by pooling from 10 to 500 recombinant progeny and sequencing to a relatively high depth, a linked region between 0.5 and 5 Mb in size as well as the responsible mutation can be identified (Schneeberger *et al.* 2009; Cuperus *et al.* 2010; Doitsidou *et al.* 2010; Zuryn *et al.* 2010; Austin *et al.* 2011; Uchida *et al.* 2011). Similarly, WGS of individual mutant mice (Arnold *et al.* 2011) or human patients with genetic disorders (Sobreira *et al.* 2010) has led to the identification of causative mutations. However, in the case of mice and humans, prior knowledge of linkage was necessary to determine which of the many sequence variants identified in the genome were associated with the phenotype.

Mapping mutants by performing WGS has not yet been applied to zebrafish. One prohibitive factor has been the high cost of sequencing an entire zebrafish genome (~1.5 Gb,

doi: 10.1534/genetics.111.136069
Manuscript received October 24, 2011; accepted for publication November 24, 2011
Supporting information is available online at http://www.genetics.org/content/suppl/2011/12/14/genetics.111.136069.DC1.

[1] These authors contributed equally to this work.

[2] Corresponding author: Department of Genetics, Harvard Medical School, and Orthopedic Research Laboratories, Children's Hospital Boston, Enders 260.2, 300 Longwood Ave., Boston, MA 02115. E-mail: harris@genetics.med.harvard.edu

compared to 100 Mb for *C. elegans* and 120 Mb for *A. thaliana*). However, new sequencing platforms have increased the throughput of sequencing and reduced its cost, now making it practical to obtain low-coverage sequence data of an entire zebrafish genome. A second prohibitive factor for applying WGS for mutation detection in zebrafish is the high level of inter- and intrastrain variation (Stickney *et al.* 2002; Guryev *et al.* 2006; Bradley *et al.* 2007; Coe *et al.* 2009) and the absence of a well-annotated catalog of natural variation; consequently, this makes it more difficult to determine whether a novel homozygous variant is a causative mutation or a low-frequency single-nucleotide polymorphism (SNP). This contrasts with the inbred organisms for which WGS has been successfully applied (Schneeberger *et al.* 2009; Cuperus *et al.* 2010; Doitsidou *et al.* 2010; Zuryn *et al.* 2010; Austin *et al.* 2011; Uchida *et al.* 2011). Here, we describe the establishment of an extensive zebrafish SNP database. Using this database in combination with low-coverage (~3×) WGS, we developed a rapid and inexpensive method to efficiently map, and frequently clone, recessive mutations in zebrafish. Furthermore, the methodology described here can be used to identify genetic loci in other model organisms with larger and highly polymorphic genomes that have annotated genomes, such as rats, mice, dogs, chickens, and other fish species.

Materials and Methods

Zebrafish husbandry and strains

Zebrafish were raised and maintained as described (Nüsslein-Volhard and Dahm 2002). Mutants were identified in the 2004 ZF-MODELS screen performed at the Max-Planck Institute for Developmental Biology (MPI-EB) in Tübingen, Germany. Mutant and wild-type strains were obtained from stocks at Children's Hospital, Boston (Tü^{B}, WIK^{B}, AB, and TLF) and at the MPI-EB (Tü^{G} and WIK^{G}). The *minamoto* (*moto*^{t31533}), *welded* (*wdd*^{t31169}), *hollow* (*hlw*^{t3373}), *fruehrentner* (*frnt*^{t31786}), and *schrumpfkopf* (*sump*^{t3625}) mutants were generated in the Tü background. For mapping, the majority of mutants were outcrossed to the WIK line, except for *sump*, which was crossed to TLF. F_2 crosses were screened for the phenotype and identified mutants and siblings were frozen.

Linkage analysis

Linkage was assessed by analysis of microsatellites (SSLPs) and SNP markers on genomic DNA from single fish using standard PCR amplification and, in the case of SNPs, analysis by dideoxy capillary sequencing.

Morpholino injections

A morpholino directed against the translation initiation site of *bmp1a* (MO1) (Jasuja *et al.* 2006) was injected at a concentration of 0.3 mM into one-cell stage Tü embryos. The phenotype was assessed at 3 days postfertilization (dpf).

Genomic DNA library construction and Illumina sequencing

For each mutant or parental strain, genomic DNA from 20 adult fish was pooled (150–250 ng from each fish—also easily obtainable from larvae), and 3–5 μg was sheared to an average size of 200 bp, using Adaptive Focused Acoustics following the manufacturer's protocol (Covaris). For three samples (*wdd*, *sump*, and *frnt*), the shearing step was omitted, since the genomic DNA appeared degraded, with most fragments being <250 bp in size as assessed by electrophoresis on a 4% agarose gel. To construct DNA libraries, the DNA fragments were blunt-ended, 5′ phosphorylated, A-tailed, and ligated to adaptors as previously described (Bowen *et al.* 2011), with the exception that adaptors did not have a 3-bp barcode sequence, and the volume of AMPure XP beads used for purification was 1.4× rather than 3.0×. Phusion High-Fidelity DNA polymerase (Finnzymes) was then used to amplify 12 μl (30%) of each library, in a total of four 50-μl PCR reactions, using the "postcapture" primers described in Bowen *et al.* (2011). Eight cycles of PCR were used for *wdd* and six cycles for all other samples. Each amplified library was sequenced on one lane of an Illumina HiSeq2000, using 100-bp single-end sequencing. Since the number of reads obtained for *frnt*, Tü^{G}, WIK^{G}, and *sump* was lower than expected, one lane of GAII 100-bp single-end sequencing was also performed for each of these samples.

Illumina data analysis

Illumina sequence reads were aligned to the reference genome (version Zv9/danRer7), using Novoalign software (http://www.novocraft.com/main/index.php) with default settings and including 3′-adaptor trimming. PCR duplicates were removed using the MarkDuplicates command in Picard (http://picard.sourceforge.net/). Multisample variant calling was performed for each chromosome on all samples simultaneously, using SAMtools and BCFtools. The SNPs were then filtered using the GATK VariantFiltrationWalker to exclude the following variants: (1) SNPs lying in low-complexity sequences or interspersed repeats, classified by RepeatMasker; (2) SNPs lying within 10 bp of an indel; (3) SNPs lying in a cluster of ≥3 SNPs per 10 bp; (3) SNPs with a quality score <30; (4) SNPs with a root-mean-square mapping quality of covering reads <40; and (5) SNPs with a total read depth <15 or >120. A perl script was used to exclude variants seen in <3 reads, variants not seen in both the forward and the reverse direction, variants with a tail bias <0.05, and variants that were not biallelic. Only the 7.6 million SNPs that passed these filtration steps were used for downstream analyses; of these, only a small percentage (0.25%, 18,978 SNPs) were found solely in one mutant and may represent ENU-induced variation. A perl script was written to classify the genotype of each mutant or reference strain at each of the 7.6 million "pass filter" SNP sites. Genotypes were classified as heterogeneous or homogeneous on the basis of the "BCFtools phred scaled genotype likelihood score." Sites covered by <2 reads were considered uninformative.

Table 1 Characteristics of linked intervals identified by whole-genome sequencing

Zebrafish mutant[a]	*moto*	*wdd*	*hlw*	*frnt*	*sump*
Whole-genome sequencing					
No. reads (10^6)	61	81	60	79	83
Genome coverage	2.6×	2.7×	2.8×	3.9×	4.1×
Size of the linked interval[b]					
Region of reduced heterogeneity[c]					
Physical size (Mb)	35	4	26	46	19
Genetic size (cM)	<25	<30	<25	<18	<18
Region of homogeneity[d]					
Physical size (Mb)	19	4	5	5	8
Genetic size (cM)	<14	<30	<4	<3	<11
Coding sequence coverage in linked interval[e]					
≥1 read	93%	92%	87%	95%	88%
≥2 reads	83%	77%	76%	92%	85%
Homogeneous SNPs in linked interval[f]					
Total	7640	225	1071	7783	9518
Not in dbSNP[g]	5984	223	1023	6431	9110
Noncoding	5663	207	997	6303	8687
Synonymous	229	12	17	89	287
Nonsynonymous	92	4	9	39	136
Unique[h]					
Noncoding	38	12	21	79	106
Synonymous	0	0	0	0	2
Nonsynonymous	2 (63)[i]	1 (119)	0 (22)	0 (4)	0 (7)

[a] *minamoto* (*moto*^{t31533}), *welded* (*wdd*^{t31169}), *hollow* (*hlw*^{t3373}), *fruehrentner* (*frnt*^{t31786}), and *schrumpfkopf* (*sump*^{t3625}).
[b] Intervals identified by a high mapping score; linkage was confirmed by analysis of SSLP or SNP markers.
[c] Region with a reduction in heterogeneity of at least 30% compared to the genome-wide average.
[d] Defined as a region with a >90% reduction in heterogeneity compared to the genome-wide average.
[e] Coding sequence of RefSeq and Ensembl genes.
[f] Detected homogeneous variants covered by at least two sequencing reads.
[g] Homogeneous variants not present in the publicly available SNP database (dbSNP) downloaded from Ensemble.
[h] Homogeneous variants not present in the reference strain database established in this study.
[i] The number of unique nonsynonymous mutations covered by only one sequencing read.

To determine the physical size of the 20-cM windows used to calculate the mapping score, the MGH mapping panel was downloaded from ZFIN (http://zfin.org/zf_info/downloads.html#marker). A script was written to obtain the Zv9 genomic coordinate of each marker from Ensembl (http://useast.ensembl.org/index.html). A genomic coordinate could be obtained for 2100 of the 3845 markers. Seventy markers mapped to more than one location and were excluded from the analysis. In addition, a BLAST search was performed to find the coordinates of some markers that did not have genomic coordinates listed in Ensembl. These markers were then used to approximate the genomic coordinate of sliding 20-cM windows throughout the genome, with a new window starting every 0.25 cM.

Annovar (http://www.openbioinformatics.org/annovar/) was used to classify variants as noncoding, synonymous, or nonsynonymous and to determine whether variants were listed in the publically available SNP database, downloaded from Ensembl (http://useast.ensembl.org/info/data/ftp/index.html). To identify variants present in only one read (which would not have been identified using SAMtools/BCFtools multisample variant calling), the SAMtools mpileup command was performed on all mutants and reference strains, for all coding exons, and a perl script was used to select variants unique to each mutant. All perl scripts, as well as aligned sequence files for each wild-type strain, are available online at http://www.fishyskeleton.com.

Results

Sequencing libraries generated from pooled DNA

We performed WGS on five previously uncharacterized mutants isolated in an ENU mutagenesis screen for adult phenotypes (ZF-MODELS; Tübingen, Germany, 2004). These recessive mutants, generated in the Tü background, were outcrossed to a polymorphic mapping strain (WIK or TLF) (Supporting Information, Figure S1); progeny from F_1 intercrosses were phenotyped and frozen for analysis. We pooled DNA from 20 affected F_2 fish from each mutant, mixing, when possible, individuals from several independent F_1 intercrosses. The F_2 fish used often stemmed from either one or two parental (P_0) crosses for a particular mutant, thus limiting the total genomic variation within a pool. Whole-genome sequencing was performed on genomic DNA libraries constructed from each mutant pool, resulting in between 60 and 83 million 100-bp reads per library (Table 1). We obtained between 2.6× and 4.1× coverage of the genome per mutant, after excluding 2–9% of the reads that were potential PCR duplicates (reads with identical 5′-end coordinates) and ~25% of reads that failed to map to unique locations in the reference genome (Zv9).

We also sequenced the genomes of four routinely used wild-type strains to establish a database of existing SNP variation. This information enabled us to predict the parental origin of SNP alleles in our mutant pools. Tü and WIK strains are commonly used in laboratories around the world. To assess the diversity among parental strains, we generated WGS from lines maintained at Children's Hospital Boston (Tü^B and WIK^B) and the Max Planck Institute in Tübingen, Germany (Tü^G and WIK^G). DNA libraries, constructed from pooled DNA from 20 fish for each of the Tü^B, WIK^B, Tü^G, WIK^G, TLF, and AB lines, were sequenced and 3.8× to 5.1× average genome coverage was obtained (Table S1).

Establishment of a reference SNP database

With low-coverage sequencing of pooled DNA, it is challenging to distinguish true SNPs from sequencing errors as many variants are represented by only a single sequencing read. However, if the same variant is observed in more than one strain, it is more likely to be a real SNP than a sequencing error. Therefore, to enhance the accuracy of SNP detection we combined the WGS data from all wild-type strains and mutants, resulting in 50× genome coverage, and then selected only the variants that were present in at least three reads for inclusion in our SNP database (see *Materials and Methods* for filtering criteria). Although variants present in only one or two reads in the combined data could also represent real SNPs, many are likely to represent sequencing errors or alignment artifacts and therefore were not included in the database.

In total, we identified a set of 7.6 million SNPs (http://www.fishyskeleton.com), which is substantially greater than the 0.7 million zebrafish SNPs currently annotated in publically available databases. Of the SNPs in public databases, 85% were detected in at least one read in our sequence data, and 45% had been included in our SNP database since they met all filtering criteria (such as being present in at least three reads). Importantly, 7.3 million of the SNPs we identified were not previously annotated, thus vastly expanding our knowledge of genetic variation in zebrafish. Using the individual WGS data from pooled DNA for each mutant and wild-type strain, we were then able to classify each SNP within that sequence as being either heterogeneous (at least one read representing each SNP allele was observed) or homogeneous (all reads represented the same allele). In each pool, an average of ~2 heterogeneous and ~3 homogeneous SNPs were observed per kilobase of genomic sequence (Table S2).

Identification of strain-specific diversity

To allow us to predict the parental origin of alleles in mutant pools, which facilitates mapping based on homozygosity-by-descent, we identified alleles that differed between parental strains. In the 7.6 million total SNPs identified, an alternate allele (with respect to the Zv9 reference genome, which is based on the Tü strain) was observed at 3–4 million sites in each wild-type line (Table S1). Consistent with previous reports noting a high degree of variation within each zebrafish strain (Stickney *et al.* 2002; Guryev *et al.* 2006; Bradley *et al.* 2007; Coe *et al.* 2009), the vast majority of these sites were heterogeneous (*i.e.*, had reads representing both the reference and the alternate alleles) (Table S1). Thus, to identify SNPs that differed between lines, we selected SNPs at which all reads represented the reference allele in one line, while the other line had at least one read representing an alternate allele. When only the SNPs with sequence coverage in all six lines (5.2 million) were considered, any two lines differed at ~40% of loci (Figure S2A), which is in agreement with previous estimates of interstrain diversity (Stickney *et al.* 2002). The majority (72%) of SNPs were shared by at least three lines, while only 11% were unique to a single line (Figure S2B). For use in our mapping studies, we selected all sites at which alternate alleles were present in the strain used for outcrossing (TLF or WIK), but not in the strain used for mutagenesis (Tü). These alternate alleles were referred to as "mapping strain alleles" and consisted of 0.74 million and 1.2 million alleles for the TLF and WIK strains, respectively (Figure S2, C and D). In each mutant pool, these sites were analyzed for the presence or absence of the mapping strain allele (Table S2).

Mapping mutants using homozygosity-by-descent

We next mapped each mutant on the basis of homozygosity-by-descent. For each mutant pool, we scanned the WGS data for regions with two characteristics: having a reduced level of heterogeneity and a reduced level of SNPs originating from the outcrossed strain, relative to the genome-wide averages of these measures. To quantify these characteristics, we designed an algorithm that produced a "mapping score," using sliding windows throughout the genome (Figure 1). Since we expected a characteristic footprint to span at least 10 cM on either side of the causative mutation (Figure S1), a window size of 20 cM, tiled at 0.25-cM intervals, was utilized. We based the window size on genetic distance (centimorgans) rather than physical distance (megabases), to take local recombination rates into account. This makes the analysis more accurate in regions close to centromeres and telomeres. Once regions with high mapping scores were identified for a particular mutant, we independently tested linkage to these regions by the use of SSLP or SNP markers on DNA pools as well as in individual progeny (Table S3). In each of the five mutants analyzed, we confirmed that the region with the highest mapping score was linked to the mutation (Figure 1).

In some cases, other unlinked areas exhibited relatively high mapping scores. We postulate that these regions represent haplotype blocks that were, by chance, shared by the two parental fish used for the initial mapping cross. We asked whether these shared haplotype blocks could have been predicted on the basis of the WGS of the parental strains, but found that each block occurred in a region in which heterogeneous SNPs (and therefore more than one haplotype) were observed in each of the parental strains. Furthermore, these blocks occurred in different locations in each mutant analyzed. Thus, if multiple regions with a high mapping score are obtained, independent tests for linkage will be needed to distinguish shared haplotype blocks from the region linked to the causative mutation. The presence of multiple high mapping scores in the genome could also represent second-site modifiers of the phenotype. These regions

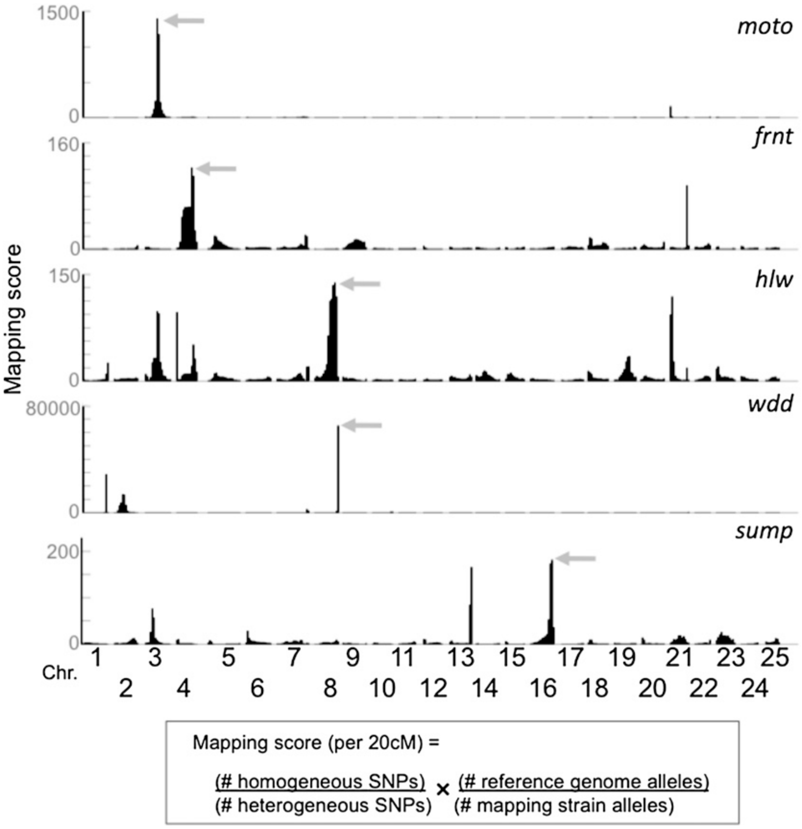

Figure 1 Mapping zebrafish mutants based on homozygosity-by-descent. Individual graphs depict the mapping scores along each chromosome for the five different mutants (*moto*, *frnt*, *hlw*, *wdd*, and *sump*). The mapping score is calculated as the ratio of homogeneous to heterogeneous SNPs, multiplied by the ratio of reference alleles to mapping strain alleles in sliding windows. The size of the sliding windows is 20 cM with an overlap of 19.75 cM between adjacent windows. Physical distances were converted to genetic distances using markers from the MGH meiotic map that have been mapped onto the Zv9 reference genome. In each of the five mutants, the region with the highest mapping score in the genome (shaded arrows) was subsequently confirmed as containing the linked interval, using SSLP or SNP markers.

could then be analyzed for sequence variants that alter the expressivity of the mutant phenotype.

Our approach has two major differences from those previously used to map *C. elegans* and *A. thaliana* mutants (Schneeberger *et al.* 2009; Cuperus *et al.* 2010; Doitsidou *et al.* 2010; Zuryn *et al.* 2010; Austin *et al.* 2011; Uchida *et al.* 2011). First, our analysis is based on genetic rather than physical distance. Second, we combine the levels of homogeneity and strain-specific SNP signatures to map the locus. We find that this analytical method provides a robust and reliable means to correctly map the region linked to the mutation in zebrafish (Figure S3 and Figure S4).

The genetic architecture of linked regions

We further refined the linked interval by identifying an area of homogeneity within the broader region defined by our mapping algorithm. Since 20 fish were pooled for each mutant, we expected the region of homogeneity to span, on average, 2.5 cM on either side of the causative mutation (one recombinant per 40 meioses). Because of the low resolution of the genetic map, we utilized 100-kb windows (rather than centimorgans) to facilitate fine mapping of the interval. Assuming random sampling of alleles with only ~3× coverage, we expected and confirmed that linked regions containing two recombination events had an ~81% reduction in heterogeneity compared to unlinked regions, while regions containing one recombination event had a reduction in heterogeneity of ~90% (Figure 2 and Figure S1). We found that regions without recombination events were almost, but not completely, homogeneous, likely due to false positive variants resulting from sequencing errors or alignment artifacts. Therefore, we defined a candidate region of homogeneity as having a reduction in heterogeneity >90%. This approach allowed us to narrow down the candidate interval in each mutant to a region between 4 and 19 Mb in size (Table 1).

Identifying candidate phenotype-causing mutations within linked intervals

One of the powerful aspects of WGS is that it provides a large amount of sequence information throughout the candidate interval, allowing for the exclusion of much of the sequence in the interval as harboring the causative mutation. Additionally, the sequence allows the potential to identify the causative change. In the five mutants analyzed, between 76% and 92% of the coding sequence within the candidate interval was covered by at least two sequencing reads (Table 1). We identified hundreds to thousands of homogeneous variants in each candidate interval, of which between 4 and 136 were predicted to be nonsynonymous. However, we could exclude most of these variants as being causative for the phenotype since we also observed them in the WGS from the other unaffected strains (Table 1). In two of the five mutants we identified the likely causative mutation as a nonsynonymous change covered by at least two reads; these particular changes are predicted to encode nonsense alleles. In the three other mutants, unique nonsynonymous changes covered by two or more reads were not detected, but between 7 and 22 nonsynonymous changes were present in sequences covered by

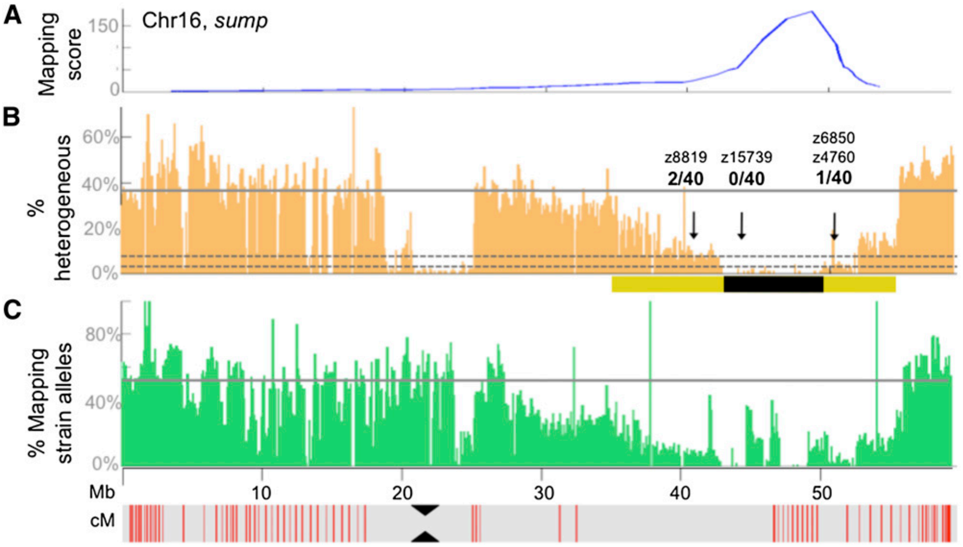

Figure 2 Genetic architecture of SNP diversity at a linked interval. (A) Graph of the mapping score across chromosome 16 in the *sump* mutant. This chromosome contained the highest mapping score in the genome. (B) Graph depicting the percentage of SNPs that were classified as heterogeneous in nonoverlapping 100-kb windows along chromosome (Chr)16. The solid gray line indicates the genome-wide average for SNPs classified as heterogeneous. Dotted gray lines indicate reductions in SNP heterogeneity of 90% (bottom line) and 81% (top line), respectively, compared to the genome-wide average. The yellow bar demarcates the region with a reduction in heterogeneity of at least 30%, while the black bar demarcates the candidate region, defined by a reduction in heterogeneity of >90%. Black arrows indicate the locations of SSLP markers used to confirm linkage to this interval by individually genotyping the 20 *sump* mutants that had been pooled for WGS. The fraction of recombination events per 40 meioses for each SSLP marker is indicated. (C) Graph showing the percentage of sites containing mapping-strain alleles, in nonoverlapping 100-kb windows along the chromosome. This percentage is calculated only for sites at which the strain used for mapping (WIK) showed an allele that was not observed in the strain used for mutagenesis (Tü). The gray line indicates the genome-wide average of the percentage of sites containing mapping-strain alleles. Physical distances in megabases along Chr16 are indicated. The red vertical lines in the gray bar below the graphs indicate genetic distances, with lines spaced at ~1-cM intervals. The position of the centromere is indicated by black triangles.

one read (Table 1). Further studies will be required to determine whether these single-read variants represent sequencing errors, normal variation, or phenotype-causing mutations.

A benefit of having performed WGS is, apart from being able to map the mutation in all mutants analyzed and to identify candidate coding mutations, that >87% of the coding sequence within the interval could be excluded because it did not differ from the reference data set. A second benefit of having performed WGS is that homogeneous SNPs identified in the candidate interval can serve as markers to test for linkage in additional F_2 fish, which will allow one to further refine the candidate interval.

The nonsynonymous changes we identified in the *welded* (*wdd*^{t31169}) and the *minamoto* (*moto*^{t31533}) mutants exemplify the value of the WGS method. For the *moto* mutant, characterized by defective spermatogenesis, two nonsynonymous mutations (Table 1), covered by two and three reads respectively, were identified within the linked interval, one missense and one nonsense mutation. The nonsense mutation was confirmed to be homozygous in all 20 fish sequenced. This mutation lies within a novel gene (*ENSDARG00000090664*) that is conserved in vertebrates. Consistent with the observed spermatogenesis defects in the mutants, this gene is expressed in testes among vertebrates (http://www.ncbi.nlm.nih.gov/unigene) and thus is a strong candidate for causing the *moto* phenotype. For the *wdd* mutant, characterized by its adult craniofacial phenotype, only one nonsynonymous change, which was supported by eight reads, was detected in the linked interval (Table 1). This change creates a nonsense mutation (p. R227X) in the gene encoding Bone morphogenetic protein 1a (Bmp1a). PCR amplification and capillary dideoxy sequencing of the genomic region in individual F_2 mutants and siblings confirmed the mutation and linkage to the mutant phenotype (0 recombinants in 66 meioses). It previously had been shown that morpholino-mediated reduction of Bmp1a function in zebrafish impairs larval development, leading to a wavy fin fold phenotype (Jasuja *et al.* 2006). We detected a similar larval fin phenotype in *wdd* mutants and confirmed that this phenotype occurs in wild-type embryos injected with a morpholino targeting the translation initiation site of *bmp1a* (Figure 3). Thus we show that the nonsense mutation in *bmp1a* is the likely causative mutation underlying the *wdd* phenotype. With a causative mutation in hand, it is now possible to investigate the mechanistic basis of this skeletal phenotype.

Minimum genome coverage needed for mapping

Our analysis showed that ~3× genome coverage was sufficient to correctly map each mutant to a defined interval, to cover >87% of coding sequence within the candidate interval, and to identify a manageable number of variants as being potential causative mutations. To determine whether lower genome coverage would be sufficient for mapping and mutation detection, we applied the same mapping algorithm to randomly selected subsets of the total sequence reads obtained for each mutant. Utilizing only 5 million reads, which is equivalent to ~0.2× genome coverage, we could still reliably identify the linked regions (Figure 4 and Figure S5). However, with 0.2× genome coverage, only 5% of coding sequence in the linked interval was covered by ≥2 reads, and 73% was not sequenced at all (Figure 4). Thus, using this method, it is feasible to map multiple mutants simultaneously by barcoding ~14 mutant DNA libraries and then sequencing a pool of these libraries on a single lane of an Illumina HiSeq apparatus. However, with this "bulk

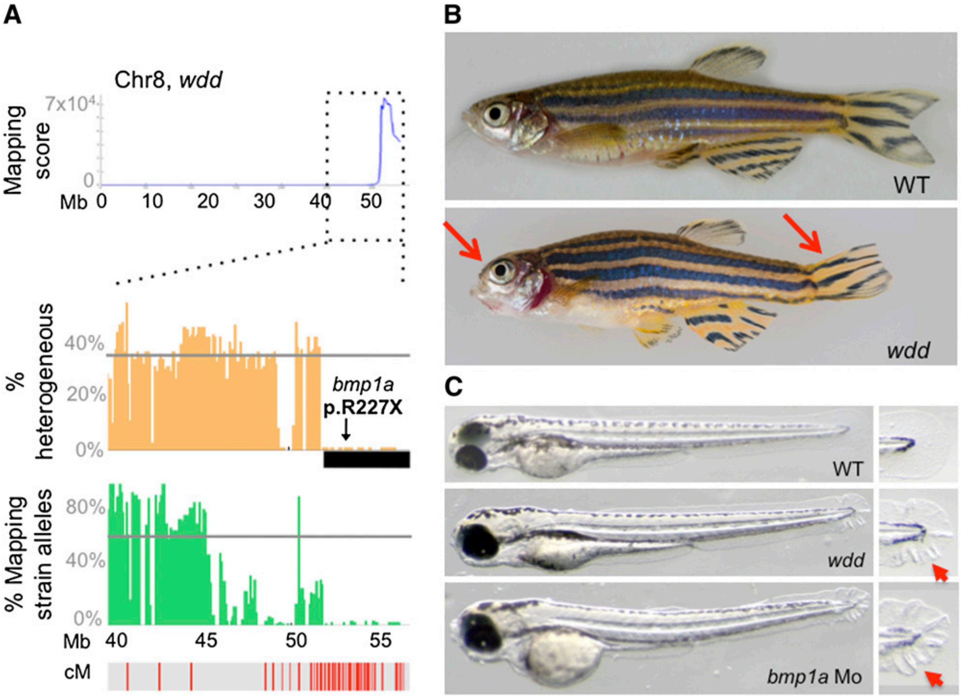

Figure 3 Identification of a loss-of-function allele of Bmp1a that underlies the *wdd* mutant phenotype. (A) The mapping-score plot for *wdd* is shown for Chr8, which contained the highest mapping score in the genome. In the graphs below, the genetic architecture of the linked region is shown. Annotation is similar to Figure 2. The location of the nonsense mutation within *bmp1a* that lies in the candidate interval is indicated (arrow). (B) Lateral view of adult wild-type and homozygous *wdd* mutant fish. Mutant fish are characterized by frontonasal shortening of the skull and deformed tailfins (red arrows). (C) Lateral view of wild-type, *wdd* mutant, and *bmp1a* morpholino-injected larvae. Mutant and morphant larvae show a similar characteristic wavy appearance of their fin folds (red arrowheads) at 3 dpf, which is not observed in wild-type larvae. Insets show a higher magnification of the distal part of the finfold.

mapping" approach it would be unlikely to identify the causative mutations using the generated sequence alone.

Discussion

We show that recessive zebrafish mutations can be efficiently mapped and cloned using low-coverage WGS of only 20 pooled mutant progeny. While WGS has been used in other experimental models, such as *C. elegans* and *A. thaliana* (Schneeberger *et al.* 2009; Cuperus *et al.* 2010; Doitsidou *et al.* 2010; Zuryn *et al.* 2010; Austin *et al.* 2011; Uchida *et al.* 2011), the size and polymorphic diversity of the zebrafish genome posed unique challenges. By constructing an extensive SNP database using WGS from six different wild-type lines, we

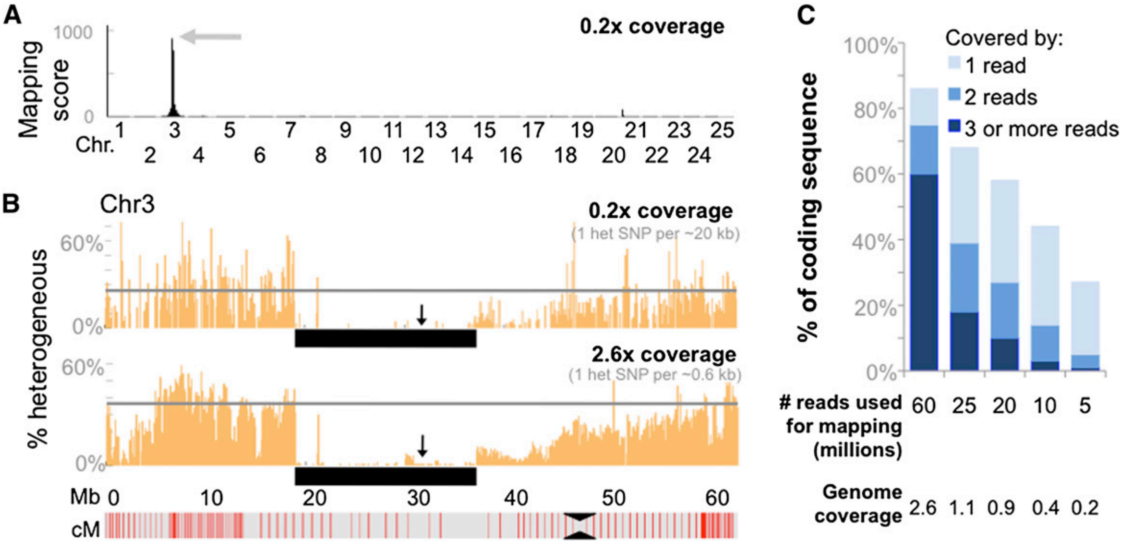

Figure 4 Mapping of mutants using only ~0.2× genome coverage. (A) Graph depicting the genome-wide mapping score plot for the *moto* mutant generated with a randomly selected subset (5 million) of the total sequencing reads, which results in a genome coverage of 0.2×. (B) Graph depicting the percentage of SNPs that were classified as heterogeneous in nonoverlapping 100-kb windows along Chr3. The arrow indicates the location of a SNP marker that was used to confirm linkage (0 recombinants in 40 meioses). While the overall number of detectable heterogeneous SNPs is reduced with a genome-wide coverage of only 0.2×, the boundaries of the linked interval can be identified just as well as with 2.6× coverage. The black bar underlies the region of homogeneity. (C) Graph depicting the loss in coverage of coding sequence that occurs as genome-wide coverage decreases.

increased the accuracy of mapping as well as the ability to distinguish phenotype-causing mutations from previously unannotated SNPs. This newly identified SNP database, containing millions of SNPs, is an order of magnitude larger than the SNPs previously annotated within publically available databases. This large database allowed us to identify strain-specific SNP signatures, which facilitated our detection of intervals that were homozygous-by-descent.

An alternative strategy of mapping mutants using WGS would be to separately sequence pools of mutants and unaffected siblings, rather than using a comparison to wild-type strains. With the limited recombination rate within the 20 fish sequenced, both strategies would provide similar resolution of the mapping interval. Using a sequence data set representing ∼50× coverage, we increase the accuracy of identifying SNPs within the mapping interval without the need for low-coverage sequence data from siblings. Additionally, analysis of the siblings for each mutant would double the cost per mutant analyzed. We think that the strain-specific and reference SNP databases we created provide a more efficient means of analyzing sequence data from multiple mutants in parallel. This SNP data set can be utilized by a large number of researchers to facilitate mapping of mutants (data and scripts available at http://www.fishyskeleton.com).

It is important to note that the detection of candidate mutations depends not only on the genome coverage obtained by WGS, but also on the quality and extent of the genome assembly that is used as a reference; in regions with poor genome assembly, lack of detection of a causative mutation will not be remedied by higher sequencing depth. Further improvements in assembly of the zebrafish genome, in the SNP database, and in massively parallel sequencing will enhance the sensitivity and specificity of our mapping approach. At present, low-coverage WGS using pooled DNA samples provides a fast and efficient means for mapping and identifying recessive mutations in zebrafish, allowing for more timely determination of altered gene function and systematic analysis of genetic regulation of vertebrate development and physiology.

Acknowledgments

We thank Iris Koch, Ursula Schach, Jennifer Zenker, Brigitte Walderich, and Hans-Georg Frohnhoefer at the Max-Planck Institute Tübingen as well as Christian Lawrence and Jason Best at the Children's Hospital Boston facilities for help with maintaining and providing fish from their respective facilities. The authors also thank David R. Beier, at Brigham and Women's Hospital Boston, for discussions and sharing unpublished ideas and Tom Carney at the Institute of Molecular and Cell Biology, Singapore, for discussion about his unpublished work on *bmp1*. M.E.B. is an Albert J. Ryan Fellow. M.L.W. is an investigator with the Howard Hughes Medical Institute. M.P.H is supported by a Glenn Foundation Award and a New Scholars Award from the Ellison Medical Foundation.

Literature Cited

Arnold, C. N., Y. Xia, P. Lin, C. Ross, M. Schwander *et al.*, 2011 Rapid identification of a disease allele in mouse through whole genome sequencing and bulk segregation analysis. Genetics 187: 633–641.

Austin, R. S., D. Vidaurre, G. Stamatiou, R. Breit, N. J. Provart *et al*, 2011 Next-generation mapping of Arabidopsis genes. Plant J. 67: 715–725.

Bowen, M. E., E. D. Boyden, I. A. Holm, B. Campos-Xavier, L. Bonafe *et al.*, 2011 Loss-of-function mutations in PTPN11 cause metachondromatosis, but not ollier disease or maffucci syndrome. PLoS Genet. 7: e1002050.

Bradley, K. M., J. B. Elmore, J. P. Breyer, B. L. Yaspan, J. R. Jessen *et al.*, 2007 A major zebrafish polymorphism resource for genetic mapping. Genome Biol. 8: R55.

Coe, T. S., P. B. Hamilton, A. M. Griffiths, D. J. Hodgson, M. A. Wahab *et al.*, 2009 Genetic variation in strains of zebrafish (danio rerio) and the implications for ecotoxicology studies. Ecotoxicology 18: 144–150.

Cuperus, J. T., T. A. Montgomery, N. Fahlgren, R. T. Burke, T. Townsend *et al.*, 2010 Identification of MIR390a precursor processing-defective mutants in Arabidopsis by direct genome sequencing. Proc. Natl. Acad. Sci. USA 107: 466–471.

Doitsidou, M., R. J. Poole, S. Sarin, H. Bigelow, and O. Hobert, 2010 C. elegans mutant identification with a one-step whole-genome-sequencing and SNP mapping strategy. PLoS ONE 5: e15435.

Geisler, R., G. J. Rauch, S. Geiger-Rudolph, A. Albrecht, F. van Bebber *et al.*, 2007 Large-scale mapping of mutations affecting zebrafish development. BMC Genomics 8: 11.

Guryev, V., M. J. Koudijs, E. Berezikov, S. L. Johnson, R. H. Plasterk *et al.*, 2006 Genetic variation in the zebrafish. Genome Res. 16: 491–497.

Jasuja, R., N. Voss, G. Ge, G. G. Hoffman, J. Lyman-Gingerich *et al.*, 2006 Bmp1 and mini fin are functionally redundant in regulating formation of the zebrafish dorsoventral axis. Mech. Dev. 123: 548–558.

Nüsslein-Volhard, C., and R. Dahm, 2002 *Zebrafish: A Practical Approach*. Oxford University Press, Oxford.

Schneeberger, K., S. Ossowski, C. Lanz, T. Juul, A. H. Petersen *et al.*, 2009 SHOREmap: simultaneous mapping and mutation identification by deep sequencing. Nat. Methods 6: 550–551.

Sobreira, N. L., E. T. Cirulli, D. Avramopoulos, E. Wohler, G. L. Oswald *et al.*, 2010 Whole-genome sequencing of a single proband together with linkage analysis identifies a Mendelian disease gene. PLoS Genet. 6: e1000991.

Stickney, H. L., J. Schmutz, I. G. Woods, C. C. Holtzer, M. C. Dickson *et al.*, 2002 Rapid mapping of zebrafish mutations with SNPs and oligonucleotide microarrays. Genome Res. 12: 1929–1934.

Uchida, N., T. Sakamoto, T. Kurata, and M. Tasaka, 2011 Identification of EMS-induced causal mutations in a non-reference Arabidopsis thaliana accession by whole genome sequencing. Plant Cell Physiol. 52: 716–722.

Zuryn, S., S. Le Gras, K. Jamet, and S. Jarriault, 2010 A strategy for direct mapping and identification of mutations by whole-genome sequencing. Genetics 186: 427–430.

Communicating editor: M. Johnston

GENETICS

Supporting Information
http://www.genetics.org/content/suppl/2011/12/14/genetics.111.136069.DC1

Efficient Mapping and Cloning of Mutations in Zebrafish by Low-Coverage Whole-Genome Sequencing

Margot E. Bowen, Katrin Henke, Kellee R. Siegfried, Matthew L. Warman, and Matthew P. Harris

DOI: 10.1534/genetics.111.136069

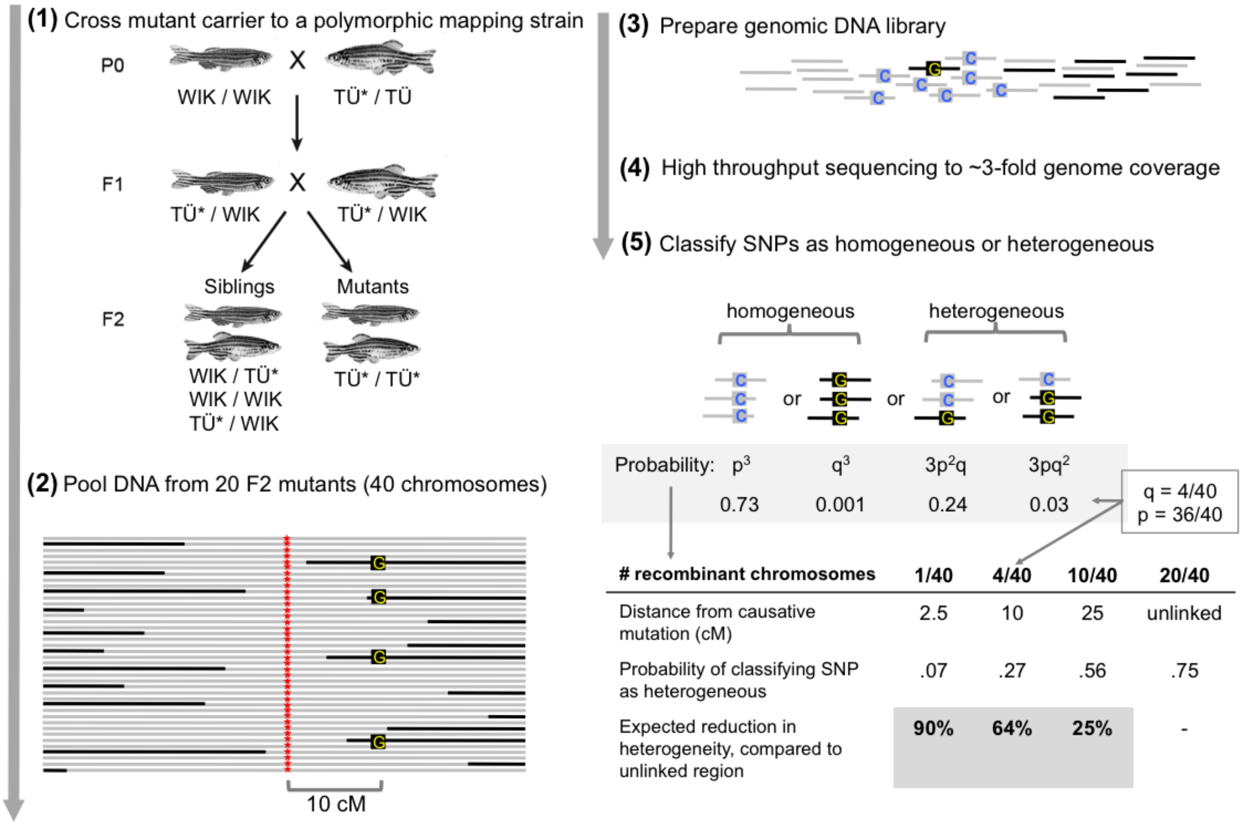
(1) Cross mutant carrier to a polymorphic mapping strain
P0
WIK / WIK
X
TÜ* / TÜ
F1
TÜ* / WIK
X
TÜ* / WIK
F2
Siblings
Mutants
WIK / TÜ*
WIK / WIK
TÜ* / WIK
TÜ* / TÜ*
(2) Pool DNA from 20 F2 mutants (40 chromosomes)
G
10 cM
(3) Prepare genomic DNA library
C
G
(4) High throughput sequencing to ~3-fold genome coverage
(5) Classify SNPs as homogeneous or heterogeneous
homogeneous
heterogeneous
C
or
G
or
C
or
G
q = 4/40
p = 36/40

Probability:	p³	q³	3p²q	3pq²
	0.73	0.001	0.24	0.03

# recombinant chromosomes	1/40	4/40	10/40	20/40
Distance from causative mutation (cM)	2.5	10	25	unlinked
Probability of classifying SNP as heterogeneous	.07	.27	.56	.75
Expected reduction in heterogeneity, compared to unlinked region	90%	64%	25%	-

Figure S1 Outline and predicted sensitivity of the approach. (**1**) The generation of fish used in mapping is accomplished by crossing identified mutants carrying a recessive ENU-induced mutation (*) within the Tü background, to a polymorphic mapping strain, (e.g., WIK). Mutant carriers (Tü*/WIK) of the F1 generation are then intercrossed to generate F2 progeny. These F2 fish are sorted based on the presence or absence of the mutant phenotype. (**2**) DNA is prepared from 20 F2 mutant progeny (Tü*/Tü*) and pooled in equal quantities. The diagram depicts the 40 chromosomes containing a phenotype-causing ENU-induced mutation (red asterisk) among the 20 mutant fish. The mutation is linked to genomic sequence originating from the Tü strain used for mutagenesis (grey fragments). Recombinants having sequence originating from the outcross strain (black fragments) can be observed at different distances from the causative mutation as a result of meiotic recombination during meiosis in the F1 generation. In a SNP located ~10 cM from the causative mutation, we expect by definition, 4 of the 40 mutation-containing chromosomes to show a mapping strain allele (G in WIK; black square) as a result of meiotic recombination. (**3**) Physical fractionation of DNA from the 20 mutant fish produces DNA fragments, that contain the aforementioned SNP (boxed C for the Tü and G for the WIK alleles), (**4**) Whole genome sequencing of the fragmented DNA library is performed on a single lane of an Illumina HiSeq platform resulting in ~3x genome coverage. (**5**) Probability for detecting a SNP as being homogenous or heterogeneous in pooled DNA from 20 mutant fish sequenced to 3x coverage. SNPs are classified as homogeneous if all 3 reads covering the SNP represent the same allele (probability = $p^3 + q^3$) and as heterogeneous if both alleles are represented (probability = $3p^2q + 3pq^2$). In an unlinked region, where both alleles are equally represented (q = 0.5; p = 0.5), the probability of a SNP being detected as heterogeneous is 0.75. Likewise, in regions where 10% of the chromosomes are recombinant, as in our example, statistically 4 out of 40 (q = 0.1) reads would show the mapping-strain allele (G), while 36 out of 40 (p = 0.9) would show the reference allele (C; Tü). Thus the probability of detecting the SNP in a heterogeneous state is 0.27. Therefore, the number of heterogeneous SNPs identified in such a region is expected to be ~64% lower than in an unlinked region (0.27/0.75 = 64%). Similarly, a ~90% reduction in heterogeneity is expected for regions containing 1 recombinant chromosome, while a ~25% reduction is expected for regions with 10 recombinant chromosomes. According to this analysis using low genome coverage, it would be of no added benefit to pool larger numbers of fish to increase the resolution of mapping. As the probability of detecting a single recombinant in, for example, 40 fish (80 chromosomes) would be lower than the level of detecting false positive heterogeneous SNPs and thus indistinguishable from noise.

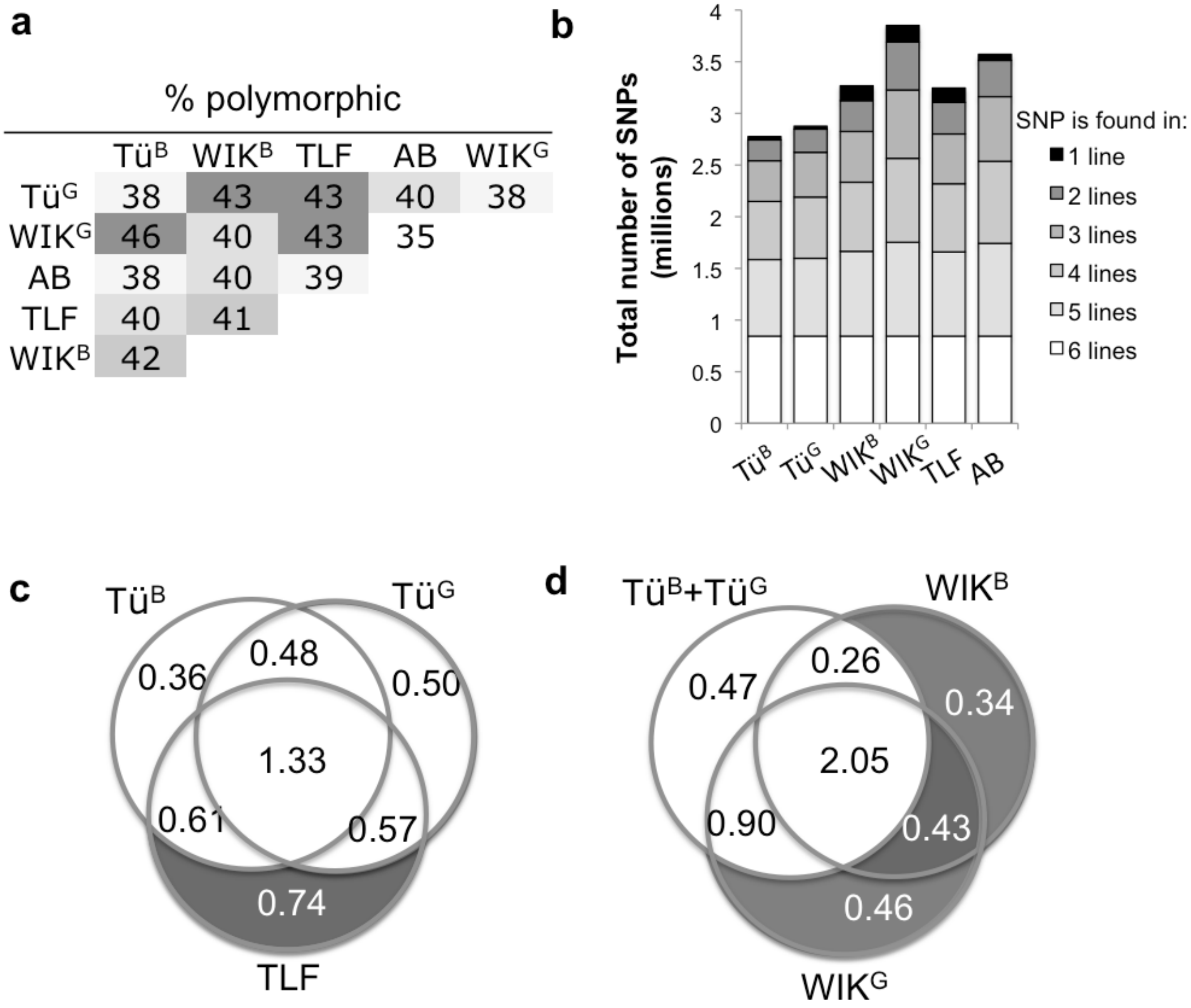

% polymorphic

	Tü^{B}	WIK^{B}	TLF	AB	WIK^{G}
Tü^{G}	38	43	43	40	38
WIK^{G}	46	40	43	35	
AB	38	40	39		
TLF	40	41			
WIK^{B}	42				

Figure S2 Genetic variation in zebrafish strains detected in low coverage WGS data of pooled DNA from 20 fish. (**a**) Pairwise comparison of SNP genotypes between parental lines showing the percentages of SNPs that are polymorphic and thus could be used to predict the parental origin for mapping based on homozygosity-by-descent. SNPs were classified as polymorphic if only the reference genome allele was observed in one line, while at least one alternate allele was observed in the second line. (**b**) Graph showing the number of polymorphic SNPs (in millions) identified in each parental line, as well as the number of lines with which these SNPs are shared. For (a) and (b), only sites with sequence coverage in all lines were considered (5.2 million sites out of the 7.6 million total SNP sites). (**c, d**) Venn diagrams showing the SNPs that were classified as mapping strain SNPs. This includes 0.74 million SNPs found in TLF but not in either of the Tü lines, and 1.2 million SNPs found in either of the WIK lines but not in either of the Tü lines. For (c) the two Tü lines are shown separately, while in (d) the data from these two lines were combined. Interestingly, due to high levels of intra-strain variation, there is a high number of SNPs that are not shared between the two Tü lines (c), and a similar number of SNPs that are not shared between the two WIK lines (d).

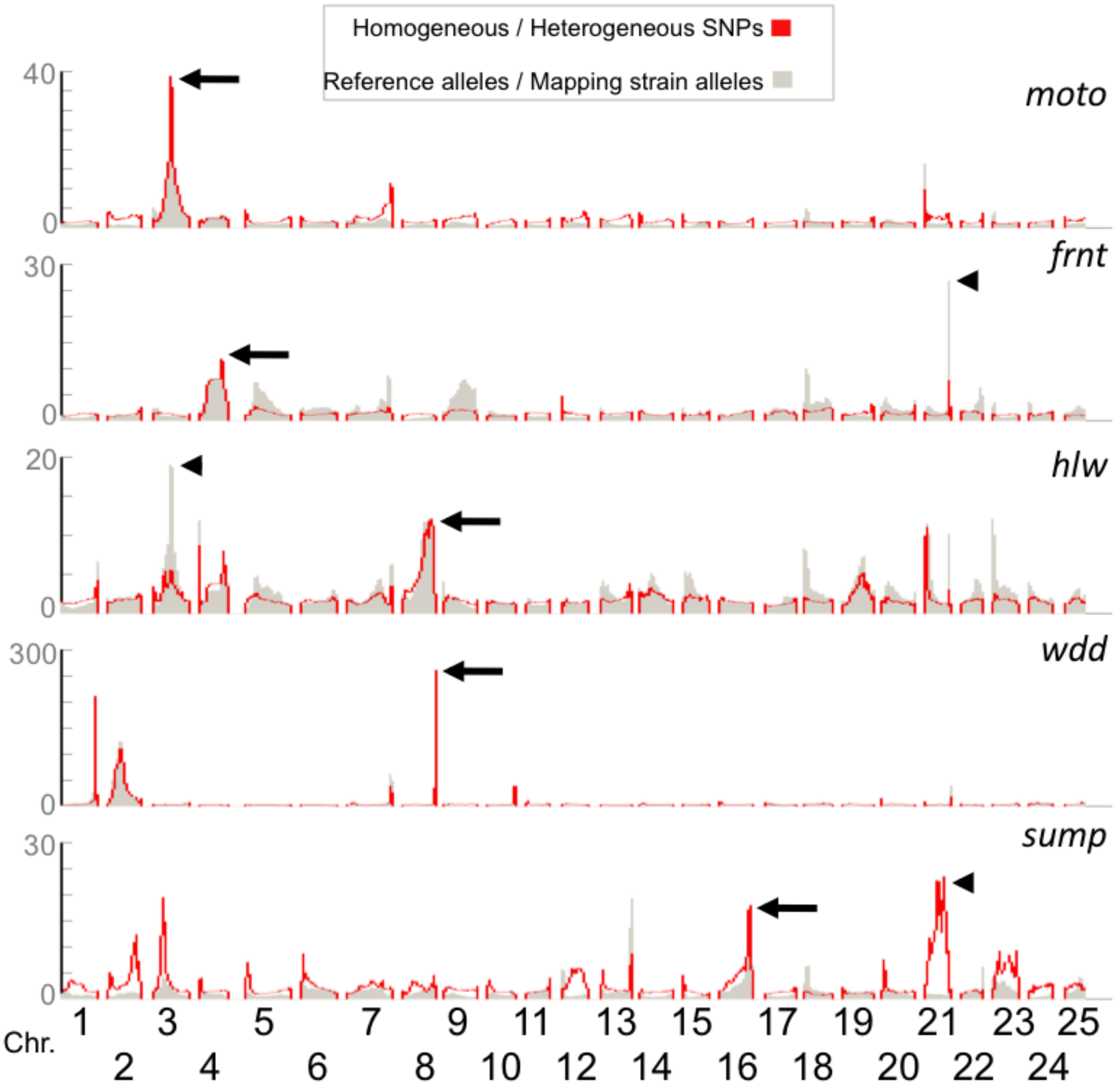

Figure S3 Mapping by combining both the frequency of heterogeneous SNPs and the frequency of mapping strain SNPs helps to eliminate false positives. Graphs show the comparison between the ratio of homogeneous to heterogeneous SNPs (red lines) to the ratio of reference genome alleles to mapping strain alleles (gray bars), for the five mutants analyzed (*moto, frnt, hlw, wdd, sump)*. Ratios were calculated for all 25 chromosomes using sliding windows of 20 cM in size, with an overlap of 19.75 cM between adjacent windows. Genetic distances were defined by the MGH meiotic map. The arrow indicates the linked region for each mutant. For three mutants (*moto, frnt, wdd*), both approaches independently predict the linked region as the region in the genome with the highest ratio. In the *hlw* and *frnt* mutants, other regions show the highest ratio of reference alleles to mapping strain alleles (arrowheads). These regions do not have a high ratio of homogeneous to heterogeneous SNPs. Similarly, for the *sump* mutant, region on Chr21 shows the highest ratio of homogeneous to heterogeneous SNPs, but this region does not have a high ratio of reference alleles to mapping strain alleles (arrowhead). Accordingly, these false positive regions would result in a lower mapping score in our combined analysis and thus would be ranked as less likely to be linked to the mutation.

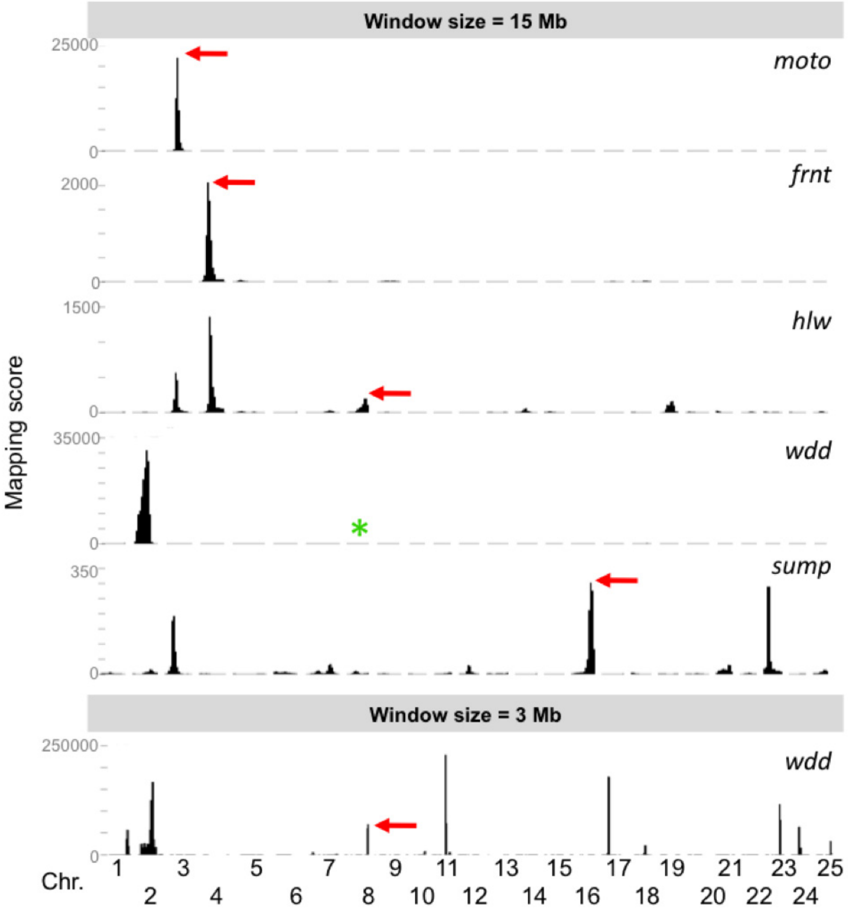

Figure S4 The sensitivity and specificity of mapping is affected by the size of the window used to calculate the mapping score. Graphs showing the genome-wide mapping scores using a sliding window of 15 Mb in size for all mutants (above), or a sliding window of 3 Mb in size for *wdd* (below), rather than the 20 cM windows used in our analysis. When 15 Mb sliding windows are used, in only three of the five mutants (*moto, frnt, sump*) the linked region is contained within the window with the highest mapping score in the genome (red arrows). In *hlw* the linked region is contained within the peak with the third highest mapping score (red arrow). In *wdd,* the linked region is not detected by an increase in the mapping score (asterisk), because the linked interval on Chr8 spans only 4 Mb. When a 3 Mb window was used for *wdd*, which should be small enough to detect the linked region, a mapping score peak appears at the linked interval (red arrow), but it is only the 5th highest peak.

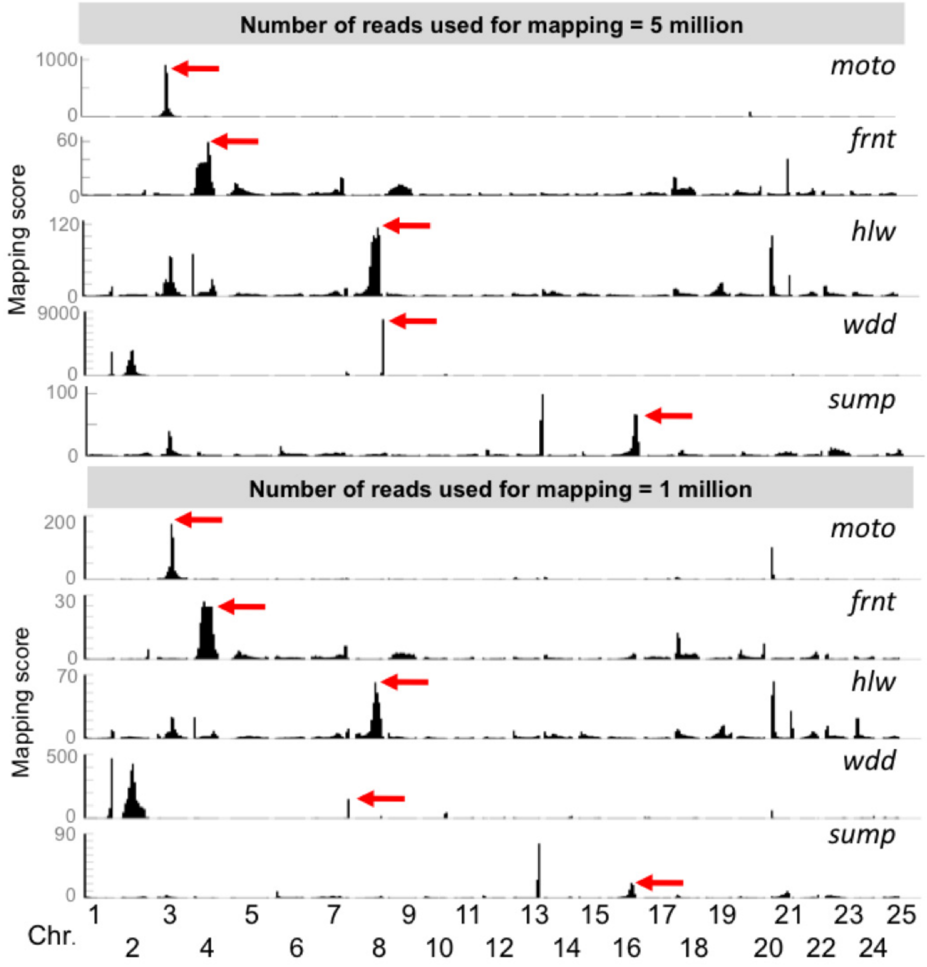

Figure S5 Minimum coverage needed for efficient mapping of zebrafish mutants. Graphs depicting the genome-wide mapping scores calculated for each mutant in 20 cM sliding windows, using either only 5 million (top) or 1 million (bottom) randomly selected Illumina sequencing reads. The actual map positions for each mutant are indicated (red arrows). When 5 million reads are used, the mapping score plots are not significantly different from those generated using all reads (>60 million) (Figure 1). The only exception is that, for *sump*, the linked region has only the 2nd highest mapping score. Even when only 1 million reads are used, in three mutants (*moto, frnt, hlw*) the linked region has the highest mapping score in the genome. For two other mutants (*wdd, sump*), the relative heights of the false positive peaks are significantly increased.

Table S1 Whole genome sequencing of pooled DNA from wild-type zebrafish strains

Wild-type pool	# reads[a] (millions)	Genome coverage	# SNPs[b] (per kb)	% het[c]
Tü^B	97	5.1x	2.6	88
Tü^G	81	4.1x	2.5	89
WIK^B	96	4.1x	2.9	64
WIK^G	81	4.0x	3.5	73
AB	90	4.6x	3.3	79
TLF	91	3.8x	2.9	56

[a]Number of 100 bp reads obtained by Illumina single end sequencing. [b]Number of positions at which at least one read representing an alternate allele was observed. Only positions at the 7.6 million SNP sites identified in this study were considered. [d]Percentage of SNPs that were heterogeneous (i.e., both reference-genome and alternate alleles were represented)

Table S2 Classifying SNPs identified by whole genome sequencing of pooled DNA from zebrafish mutants

	SNP genotype[a] (average per kb)				Parental origin of alleles[b] (average per kb)	
		Hom				
Mutant pool	Het	Non-ref	Ref	n/d	Mapping strain allele	Reference genome allele
moto	1.6	0.9	1.8	1.3	0.6	0.6
wdd	1.0	0.4	2.1	2.2	0.3	0.3
hlw	1.7	0.4	2.4	1.0	0.4	0.8
frnt	2.1	0.6	2.1	0.7	0.6	0.7
sump	1.8	1.1	2.0	0.6	0.7	0.6

[a] Calculated for the 7.6 million SNP sites identified in this study. SNPs were defined as heterogeneous (Het) for sites at which both a reference genome allele (Zv9) and an alternate allele were observed in the WGS of pooled DNA. SNPs were defined as homogeneous (Hom) for sites at which only the alternate allele (non-ref) or the reference genome allele (ref) were observed; sites that were covered by less than 2 sequencing reads were deemed uninformative (n/d). [b] Calculated for all SNP sites at which an alternate allele was present in the TLF or WIK mapping strain, but not in the Tü strain (0.7 million and 1.2 million sites respectively); Mapping strain allele = at least one read representing the alternate allele was observed in a mutant pool; Reference genome allele = all reads in a mutant pool represented the reference genome allele. Note that the reference genome is based on the Tü strain.

Table S3 SSLP and SNP marker linkage data

Zebrafish mutant	Chr[a]	Region of homogeneity (Mb)[b]	Marker[c]	Position[d] (Mb)	Recombinants/meiosis[e]
moto	3	19-36.6	z9964	34.3	2/90
wdd	8	51.8-55	*bmp1a*	53.5	0/66
hlw	8	43-47	z25210	43	2/44
			z7130	45.6	1/46
frnt	4	15-27.8	z11538	23.1	3/44
			z20450	24.4	2/44
sump	16	41.8-51.2	z8819	41.3	2/56
			z15739	43.9	0/56
			z4670	50.8	1/40
			z6854	50.6	1/40

[a]Chromosome showing the highest mapping score. [b]Interval on the chromosome showing homogeneity. [c]Marker used to confirm linkage. [d]Marker position on the Chromosome in Mb. [e]Recombinants identified for each marker in the number of meiosis tested.